Published in final edited form as:
Chembiochem. 2006 July ; 7(7): 1114–1122.

scyllo-Inositol Pentakisphosphate as an Analogue of *myo*-Inositol 1,3,4,5,6-Pentakisphosphate: Chemical Synthesis, Physicochemistry and Biological Applications

Andrew M. Riley[a], **Melanie Trusselle**[a], **Paul Kuad**[b], **Michal Borkovec**[c], **Jaiesoon Cho**[d], **Jae H. Choi**[d], **Xun Qian**[d], **Stephen B. Shears**[d], **Bernard Spiess**[b], and **Barry V. L. Potter***[a]

[a]*Dr. A. M. Riley, Dr. M. Trusselle, Prof. Dr. B. V. L. Potter, Wolfson Laboratory of Medicinal Chemistry, Department of Pharmacy and Pharmacology, University of Bath, Claverton Down, Bath, BA2 7AY (UK), Fax: (+44) 1225-386114, E-mail: B.V.L.Potter@bath.ac.uk*

[b]*Dr. P. Kuad, Prof. Dr. B. Spiess, Département de Pharmacochimie de la Communication Cellulaire, UMR 7175-LC1 du CNRS-ULP, Faculté de Pharmacie, 74, route du Rhin, B. P. 24, 67401 Illkirch Cedex (France.)*

[c]*Dr. M. Borkovec, Department of Inorganic, Analytical, and Applied Chemistry, University of Geneva, 30 Quai Ernest-Ansermet, 1211 Geneva 4 (Switzerland)*

[d]*Dr. J. Cho, Dr. J. H. Choi, Dr. X. Qian, Dr. S. B. Shears, Inositide Signaling Group, Laboratory of Signal Transduction and National Institute of Environmental Health Sciences, Research Triangle Park, NC 27709 (USA)*

Abstract

myo-*Inositol 1,3,4,5,6-pentakisphosphate (Ins(1,3,4,5,6)P_5), an inositol polyphosphate of emerging significance in cellular signalling, and its C-2 epimer* scyllo-*inositol pentakisphosphate (*scyllo-*InsP_5) were synthesised from the same* myo-*inositol-based precursor. Potentiometric and NMR titrations show that both pentakis-phosphates undergo a conformational ring-flip at higher pH, beginning at pH 8 for* scyllo-*InsP_5 and pH 9 for Ins(1,3,4,5,6)P_5. Over the physiological pH range, however, the conformation of the inositol rings and the microprotonation patterns of the phosphate groups in Ins(1,3,4,5,6)P_5 and* scyllo-*InsP_5 are similar. Thus,* scyllo-*InsP_5 should be a useful tool for identifying biologically relevant actions of Ins(1,3,4,5,6)P_5, mediated by specific binding sites, and distinguishing them from nonspecific electrostatic effects. We also demonstrate that, although* scyllo-*InsP_5 and Ins(1,3,4,5,6)P_5 are both hydrolysed by multiple inositol polyphosphate phosphatase (MINPP),* scyllo-*InsP_5 is not dephosphorylated by PTEN or phosphorylated by Ins (1,3,4,5,6)P_5 2-kinases. This finding both reinforces the value of* scyllo-*InsP_5 as a biological control and shows that the axial 2-OH group of Ins(1,3,4,5,6)P_5 plays a part in substrate recognition by PTEN and the Ins(1,3,4,5,6)P_5 2-kinases.*

Keywords

cyclitols; enzymes; inositol phosphates; protecting groups; structure—activity relationships

Introduction

myo-Inositol 1,3,4,5,6-pentakisphosphate (Ins(1,3,4,5,6)P_5, **1**; Scheme 1) which is present in nearly all eukaryotic cells at levels of 15–50 μM, has been called a signalling "hub" because it appears to serve several biological roles.[1] For example, Ins(1,3,4,5,6)P_5 has been proposed to regulate the rate of cellular proliferation,[2, 3] apoptosis,[3] viral assembly,[4] chromatin remodelling[5] and the activity of L-type Ca^{2+} channels.[6] In addition, Ins(1,3,4,5,6)P_5 inhibits

angiogenesis and blocks growth of tumour cell xenografts.[7] Ins(1,3,4,5,6)P_5 can also regulate signalling by 3-phosphorylated lipids—by binding to 3-phosphoinositide-dependent protein kinase 1 (PDK1) Ins(1,3,4,5,6)P_5 can anchor the kinase in the cytosol and prevent it from being activated by phosphatidylinositol 3,4,5-trisphosphate (PtdIns- (3,4,5)P_3).[8] Moreover, Ins (1,3,4,5,6)P_5 can competitively inhibit PtdIns(3,4,5)P_3 metabolism by phosphatase and tensin homologue deleted on chromosome ten (PTEN).[9]

It is important to understand the structural determinants of the interactions between Ins (1,3,4,5,6)P_5 and the proteins that it regulates. Such knowledge helps our understanding of basic biological processes at a molecular level, while also aiding the rational design of ligand agonists and antagonists that might have therapeutic value. The biological actions of inositol phosphates often rely on stereospecific ligand recognition by dedicated receptors. This applies, for example, to Ca^{2+} mobilization by Ins(1,4,5)P_3[10] and Cl^- channel inhibition by Ins (3,4,5,6)P_4.[11] These ligand–protein interactions involve electrostatic interactions between the protein and the negatively charged phosphate groups on the ligand. Geometric constraints imposed by the bulky nature of the phosphate groups will also contribute to ligand specificity. However, spatial restrictions will be less important if the protein's binding cleft is relatively spacious or if the ligand-binding site is on the surface of the protein. In such situations, electrostatic interactions can be delocalized, in which case ligand–protein association is driven more by the number of phosphate groups in a molecule, rather than their exact placement around the inositol ring.[12] One example of this phenomenon is the binding of inositol phosphates to pleckstrin homology (PH) domains.[12] This is a biologically relevant mechanism which could, in some cases, be exploited by a molecule such as Ins(1,3,4,5,6) P_5.[8]

Unfortunately, delocalized electrostatic interactions between inositol polyphosphates and proteins, in vitro, can drive biologically irrelevant ligand binding, especially when the experimental milieu does not appropriately imitate the situation in vivo.[13] In such cases, the apparent functional data that might emerge from such assays can be misleading. Thus, it is useful when examining the biological activity of an inositol polyphosphate to have a closely related analogue that cannot imitate the actions of the "active" parent molecule. A good example in the literature is the demonstration that *scyllo*-inositol hexakis-phosphate (*scyllo*-$InsP_6$) does not imitate the ability of *myo*-$InsP_6$ to inhibit an inwardly rectifying K^+ current in plant guard-cell protoplasts.[14] All of the phosphate groups in the naturally occurring *scyllo*-$InsP_6$ are esters of equatorial hydroxyl groups (i.e., approximately in the plane of the inositol ring). In contrast, the 2-phosphate in *myo*-$InsP_6$ is linked as an ester of an axial hydroxyl group, that is, it is perpendicular to the plane of the ring. The demonstration that *myo*-$InsP_6$, but not *scyllo*-$InsP_6$, is biologically active indicates that a receptor protein has a discriminating, stereospecific ligand-binding site, rather than merely reacting to high negative-charge density. Such specificity is often the hallmark of a biologically relevant process.

In this study, we have investigated the value of *scyllo*-inositol pentakisphosphate (*scyllo*-$InsP_5$,[15] **2**; Scheme 1), a totally synthetic molecule, as a control for studies into the biological activity of Ins(1,3,4,5,6)P_5. We describe convenient synthetic routes to both pentakisphosphates from *myo*-inositol from an orthoester intermediate and compare the physicochemical properties of the two $InsP_5$ epimers. The physicochemical part of the study was prompted by the consideration that the difference in the orientation of the hydroxyl group between the two polyphosphates might differentially affect the basicity of the adjacent phosphates through intramolecular hydrogen bonding, which in turn affects the hydration shell and association with cations.[16] Next, the metabolism of Ins(1,3,4,5,6)P_5 and *scyllo*-$InsP_5$ by two phosphatases that are known to hydrolyse Ins(1,3,4,5,6)P_5 (multiple inositol polyphosphate phosphatase (MINPP) and PTEN) was compared. Finally, we examined whether *scyllo*-$InsP_5$ can be phosphorylated by Ins(1,3,4,5,6)P_5 2-kinases.[17,18] This

highlights another reason for selecting *scyllo*-$InsP_5$ as a control polyphosphate, because *myo*-$InsP_6$ has itself drawn attention as an intracellular signal.[10,19] Thus, in experiments with cell-free systems, it would be useful when adding Ins(1,3,4,5,6)P_5, to be able to exclude effects that might arise from its phosphorylation to $InsP_6$. Moreover, an insight into the reactivity of 2-kinases towards *scyllo*-$InsP_5$ could further our understanding of the origin of *scyllo*-$InsP_6$—an enigmatic molecule of unknown metabolic origin that is nevertheless present in large quantities in soils.[20]

Results

Chemical synthesis of Ins(1,3,4,5,6)P_5 and *scyllo*-$InsP_5$

The versatile alcohol precursor **3**[21] (Scheme 2) was chosen as starting material for the synthesis of both Ins(1,3,4,5,6)P_5 and *scyllo*-$InsP_5$. Oxidation of **3** at C-2,[21] followed by stereoselective reduction by using sodium borohydride[22] exclusively gave the axial alcohol **5**. Interestingly, the fact that **5** has the *scyllo*-configuration is immediately apparent from the ^{1}H NMR spectrum, because the signal corresponding to the methylidyne proton appears as a singlet, while in the *myo*-epimer **3** it appears as a narrow doublet due to a long range ^5J spin–spin coupling to the axial H-2 proton. Benzylation of the free axial OH group in **5** gave **6** and treatment of **6** with HCl in refluxing ethanol cleaved both the orthoformate ester and the *p*-methoxybenzyl ethers. The pentaol product, 1-*O*-benzyl-*scyllo*-inositol (**7**) crystallised from the reaction mixture on cooling. Phosphitylation of **7**, followed by oxidation of phosphite esters with *m*CPBA gave fully protected **8**. Finally, hydrogenolytic deprotection of **8** gave *scyllo*-inositol pentakisphosphate (**2**),[15] which was purified by ion-exchange chromatography on Q-Sepharose fast-flow resin by using a gradient of aqueous triethylammonium bicarbonate. Ins(1,3,4,5,6)P_5[23] (**1**) was synthesised in a similar way from **3** from the 2-*O*-benzyl ether **9** (Scheme 2).

pH-dependent conformational changes of Ins(1,3,4,5,6)P_5 and *scyllo*-$InsP_5$

For inositol phosphates, the analysis of ^{31}P and ^{1}H NMR titration curves provides valuable information on both the charged species likely to be present at physiological pH and the conformational dependence of the inositol ring with respect to the ionisation states of the individual phosphate groups. NMR and potentiometric titrations of Ins(1,3,4,5,6)P_5 and *scyllo*-$InsP_5$ were performed in KCl (0.2 M) at 37 °C, a medium that mimics the ionic strength and temperature conditions encountered in the cell. To facilitate the discussion, the inositol ring in *scyllo*-$InsP_5$ will here be numbered so that the attached phosphate groups correspond with those in Ins(1,3,4,5,6)P_5, although this is a departure from the strict rules of inositol nomenclature.

The ^{31}P NMR titration curves of Ins(1,3,4,5,6)P_5 and *scyllo*-$InsP_5$ are shown in Figure 1. Due to the symmetry of the molecules, only three curves are observed for each. Their general shape differs only slightly between the two molecules. In each pentakisphosphate, P4–P6 and P5 behave similarly, and show an intermediate plateau or even a slight deshielding upon protonation, whereas P1–P3 keeps a more attenuated biphasic shape. Interestingly, the chemical shifts of the phosphorus atoms in the protonated and deprotonated species differ by more than 1.30 ppm. This, along with the broadening of the phosphorus resonances that occur for Ins(1,3,4,5,6)P_5 and *scyllo*-$InsP_5$ in the pH ranges 9–11 and 8–10 respectively, suggest the presence of an interconverting mixture of conformers with either five equatorial (lower pH) or five axial phosphate groups (higher pH).

Examination of the ^{1}H NMR titration curves for the two compounds confirmed that an inositol ring flip occurs at the earliest protonation steps. This is illustrated for *scyllo*-$InsP_5$ in Figure 2, where a marked upfield shift for the signals that correspond to the protons of the inositol ring

can be observed as the pH decreases from 10 to 8. This corresponds to the switching of the ring protons from an equatorial to an axial position. In line with this ring flip, the coupling constants between two vicinal protons in an equatorial–equatorial relationship (J_{eq-eq}, ca. 2–3 Hz) rapidly increase to 8–10 Hz; this corresponds to the couplings of two axial vicinal protons (J_{ax-ax}). The same conclusions can be drawn from ^{1}H NMR titration curves for Ins(1,3,4,5,6)P_5 (not shown), with the only difference being that the conformational transition arises in the 11 to 9 pH range. Barrientos and Murthy,[24] who thoroughly investigated the conformational preferences of inositol mono- to hexakisphosphates by ^{1}H NMR spectroscopy, also observed pH-dependent ring conformational changes for Ins(1,2,3,4,6)P_5 and Ins(1,2,3,5,6)P_5.

Protonation patterns of Ins(1,3,4,5,6)P_5 and *scyllo*-InsP_5

Quantitative information about the intrinsic acid–base character of the phosphate groups in Ins(1,3,4,5,6)P_5 and *scyllo*-InsP_5 can be drawn from both the potentiometric and the NMR titration curves. Although each inositol pentakisphosphate carries ten protonatable sites (two on each phosphate group), only five of them will accept a proton for pHs ranging from 12 down to 3. Thus, for each pentakisphosphate, six possible macrostates exist over this pH range, with total electrostatic charges ranging from −10 at pH 12 (zero protons, $n = 0$) to −5 at pH 3 (five protons, $n = 5$). The probabilities of these macrostates, calculated from the potentiometric titration curves for Ins(1,3,4,5,6)P_5 and *scyllo*-InsP_5 are shown in Figure 3. It can be seen that the pH-dependent distributions of the macrostates for the two pentakisphosphates are similar, with the triprotonated species ($n = 3$) predominating at pH 7.5 in each case.

More complex microprotonation processes, considering each phosphate group individually, were treated by analysis of the ^{31}P NMR curves by using the recently published "cluster-expansion method".[25] This analysis enables the detailed microscopic protonation patterns over the studied pH range to be calculated for each pentakisphosphate. In the present study, we are primarily concerned with the properties of Ins(1,3,4,5,6)P_5 and *scyllo*-InsP_5 under physiological conditions and so only a part of this complex pattern will be considered in each case. The conditional probabilities calculated for Ins(1,3,4,5,6)P_5 and *scyllo*-InsP_5 at pH 7.5 (Figure 4) describe the proportions of the different microspecies of each pentakisphosphate that exist at a pH close to physiological conditions. It can be observed that for Ins(1,3,4,5,6)P_5 and *scyllo*-InsP_5, the same triprotonated and tetraprotonated species predominate at pH 7.5, with small differences in their populations. Thus, under these conditions, the two pentakisphosphates are expected to behave similarly with respect to overall electrostatic properties and charge distribution.

Metabolism of Ins(1,3,4,5,6)P_5 and *scyllo*-InsP_5 by human MINPP and PTEN

One of the goals of the current study was to compare the metabolism of *scyllo*-InsP_5 and Ins(1,3,4,5,6)P_5. MINPP[26] and PTEN[9] are two inositol phosphate phosphatases that are known to be capable of actively hydrolysing Ins(1,3,4,5,6)P_5 in mammals. We found that recombinant human MINPP dephosphorylated *scyllo*-InsP_5 and Ins(1,3,4,5,6)P_5 at similar rates (9.0 ± 0.1 and 6.2 ± 0.3 nmolmg $^{-1}$min^{-1}, respectively). Therefore, the active site of MINPP does not distinguish between these two epimers of InsP_5.

In contrast, we found that recombinant human PTEN showed no detectable metabolism of *scyllo*-InsP_5, even though Ins(1,3,4,5,6)P_5 is a substrate (11.8 ± 1.3 nmolmg^{-1}min^{-1}). Furthermore, 250 μM *scyllo*-InsP_5 did not inhibit the dephosphorylation of 25 μM Ins(1,3,4,5,6)P_5 (12.1 vs. 11.6 nmol mg^{-1}min^{-1} in the absence or presence of *scyllo*-InsP_5, respectively). Thus, *scyllo*-InsP_5 would be predicted to bind less effectively than Ins(1,3,4,5,6)P_5 to the catalytic site of PTEN.

Metabolism of Ins(1,3,4,5,6)P_5 and *scyllo*-InsP_5 by Ins(1,3,4,5,6)P_5 2-kinase

We next investigated the ability of Ins(1,3,4,5,6)P_5 and *scyllo*-InsP_5 to be phosphorylated by Ins(1,3,4,5,6)P_5 2-kinase. Using recombinant enzymes from *Arabidopsis thaliana*, *Sacromyces cerevisiae* and *Homo sapiens*, we measured the incorporation of ^{32}P into each pentakisphosphate from the phosphate donor γ-^{32}P-ATP (Experimental Section). Ins(1,3,4,5,6)P_5 was readily phosphorylated by each species of 2-kinase. However, there was no detectable phosphorylation of *scyllo*-InsP_5. Furthermore, in a representative experiment with the *Arabidopsis* 2-kinase, phosphorylation of 50 μM Ins(1,3,4,5,6)P_5 was not significantly affected by the addition of 50 μM *scyllo*-InsP_5 (3621 vs. 3336 c.p.m. ^{32}P-InsP_6 formed, respectively) but 500 μM *scyllo*-InsP_5 inhibited the reaction by approximately 80 % (766 c.p.m. ^{32}P-InsP_6 formed).

Discussion

Nonspecific electrostatic interactions can introduce a difficult practical problem when exploring the mechanism of action of a highly charged molecule such as Ins(1,3,4,5,6)P_5. Some delocalized electrostatic interactions of inositol phosphates with proteins might be biologically relevant.[10,11] However, other delocalized electrostatic interactions, which can be permitted in a particular set of experimental conditions, might not be relevant to the intracellular milieu.[13]

Based on earlier studies of other inositol phosphates, a larger difference between the acid–base properties of Ins(1,3,4,5,6)P_5 and *scyllo*-InsP_5 might have been expected. For example, marked differences were previously observed between Ins(1,4,5)P_3 and *epi*-Ins(1,4,5)P_3, which has an axially orientated 6-OH group,[27] or Ins(1,4,6)P_3, which has its 2-OH and 3-OH groups in inverted configurations with regard to Ins-(1,4,5)P_3.[28] However, the physicochemical studies described above show that the protonation pattern of *scyllo*-InsP_5 parallels that of Ins(1,3,4,5,6)P_5 over the physiological pH range. Detailed analysis by using cluster expansion (not shown) suggests that this similarity between the two epimers could arise from a strong P1–P3 interaction for *scyllo*-InsP_5, which is compensated by large P1–P6 and P3–P4 interactions for Ins(1,3,4,5,6)P_5. The differences in the strengths of these interactions are presumably a sign of different hydrogen-bonding patterns for the two epimers due to the difference in orientation of the hydroxyl group. While these effects might have biological consequences if the 1,2,3 moiety of the inositol ring is important in binding to a selective binding site, their overall effect is to make the charge distribution of Ins(1,3,4,5,6)P_5 and *scyllo*-InsP_5 similar at physiological pH.

The conformation of organic molecules influences their biological activity by impacting their binding interactions with enzymes and receptors. Barrientos and Murthy[24] have shown that Ins(1,2,3,4,6)P_5 and Ins(1,2,3,5,6)P_5 undergo a pH-dependent ring flip, whereupon the substituents around the inositol ring switch from a 5-equatorial/1-axial conformation to a 1-equatorial/5-axial arrangement. The actual pH at which this conformational change occurs is strongly dependent upon the spatial placement of phosphate groups around the inositol ring. We therefore compared the influence of pH on the conformations of Ins(1,3,4,5,6)P_5 and *scyllo*-InsP_5, because these were factors that could potentially establish different biological activities for these compounds. Our results show that pH-dependent conformational changes occur for both Ins(1,3,4,5,6)P_5 and *scyllo*-InsP_5 and that the conformational change for *scyllo*-InsP_5 occurs at about one pH unit lower than that of Ins(1,3,4,5,6)P_5, with the inositol ring flip beginning at pH 8 and 9, respectively. However, the NMR titrations show that, in solution, under normal physiological conditions, Ins(1,3,4,5,6)P_5 and *scyllo*-InsP_5 will both exist in the conformation that has five equatorial phosphate groups.

The physiological relevance of the differences in conformational behaviour at higher pH for the interaction of Ins(1,3,4,5,6)P_5 and *scyllo*-InsP_5 with enzymes and receptors is more difficult to assess, because the pH and the dielectric constant in the vicinity of a protein-binding site are difficult to measure. In theory, both parameters can change the acid–base properties of the ligands with respect to the aqueous medium that was used in this study. However, with this reservation in mind, we can conclude that *scyllo*-InsP_5 will likely mimic interactions between Ins(1,3,4,5,6)P_5 and proteins that are largely based on delocalized electrostatics. Such a determination would be an important step forward from a mechanistic perspective, but additional experiments would still be necessary to determine if such interactions were to be biologically relevant. It can also be anticipated that Ins(1,3,4,5,6)P_5 will interact with certain proteins in a manner in which the precise spatial geometry of the ligand helps to dictate specificity. Such specific interactions have evolved in order to distinguish a particular inositol phosphate from the many others that cells contain. Indeed, we show in the current study that *scyllo*-InsP_5 cannot be metabolized by PTEN or by Ins(1,3,4,5,6)P_5 2-kinases.

An X-ray structure of PTEN in complex with L-(+)-tartrate is available.[29] Furthermore, the catalytic mechanism of the phosphatase activity of PTEN can be inferred[29] from studies on related protein-tyrosine phosphatases (PTPs), whose catalytic domains have sequence and structural homology with that of PTEN. We docked a flexible model of Ins(1,3,4,5,6)P_5 into a model of the PTEN binding site (see refs. [9,29] and Experimental Section) to examine which features of Ins(1,3,4,5,6)P_5 might be important for its interaction with PTEN (Figure 5). Detailed structural and mechanistic studies of PTPs[30] have shown that binding of substrates (phosphotyrosine) to their active sites induces a large conformational change which brings a flexible loop of residues (the “general acid loop” [30a]) down into the binding pocket. This generates additional stabilising interactions and allows an aspartate residue to protonate the scissile phenolic oxygen of phosphotyrosine. By applying this mechanism to the hydrolysis of Ins(1,3,4,5,6)P_5 by PTEN, our model suggests that, on binding of Ins(1,3,4,5,6)P_5 to the active site, the general acid loop would move towards the area of the binding site above the axial 2-OH group so as to approach the O-3 atom of Ins(1,3,4,5,6)P_5. Thus, one possibility is that the axial 2-OH group of Ins(1,3,4,5,6)P_5 interacts with the general acid loop—an interaction that would be impossible for the equatorial hydroxyl group of *scyllo*-InsP_5. Another possibility is that the conformation of the 1-phosphate group is influenced by intramolecular interactions with the adjacent hydroxyl group so that, in *scyllo*-InsP_5, this phosphate is not optimally positioned for binding. Our model predicts that the 1-phosphate group of Ins(1,3,4,5,6)P_5, which is equivalent to the phosphate diester in *myo*-inositol phospholipids, could interact with Lys125 of the PTEN active site (Figure 5).

In the case of Ins(1,3,4,5,6)P_5 2-kinases no X-ray structure is currently available. The human and plant Ins(1,3,4,5,6)P_5 2-kinases show some limited (27 %) sequence identity, but the human and yeast homologues are even more divergent (only 14% sequence identity). Nevertheless, in each case the active site discriminates between *scyllo*-InsP_5 and Ins(1,3,4,5,6)P_5, this suggests important similarities in the structure of this region. Our results imply that, as for PTEN, the axial 2-OH group is important for substrate recognition by 2-kinases. Considerable quantities of *scyllo*-InsP_6, are found in soils[20] and our results reinforce the enigma of the metabolic origin of this material.

Because Ins(1,3,4,5,6)P_5 and *scyllo*-InsP_5 are physicochemically similar at physiological pH, we argue that, in those experimental situations in which *scyllo*-InsP_5 does not imitate a biological action of Ins(1,3,4,5,6)P_5, then a strong case can be made that Ins(1,3,4,5,6)P_5 is acting specifically, and therefore, in a physiologically relevant manner. Moreover, the inability of *scyllo*-InsP_5 to be phosphorylated by 2-kinases could exclude the possibility that the synthesis of InsP_6 contributes to any of the effects detected in the experiment. *scyllo*-InsP_5 will not be metabolically inert in all experiments with cell extracts; in the current study we did find

it to be a substrate of MINPP. This finding is not unexpected, as MINPP is also capable of binding and hydrolysing $InsP_6$. This suggests that the active site of MINPP can tolerate modifications to the 2-hydroxyl group of Ins(1,3,4,5,6)P_5. However, in most mammalian cells MINPP is restricted to the interior of the endoplasmic reticulum and only has very limited access to cytosolic inositol phosphates such as Ins(1,3,4,5,6)P_5. Thus, there are several experimental situations, such as during the microinjection of inositol phosphates into cell cytosol or during patch-clamp experiments, in which MINPP-dependent $InsP_5$ metabolism will not be a complicating factor. In such circumstances, *scyllo*-$InsP_5$ will be metabolically inert. Overall, there are a number of experimental paradigms in which *scyllo*-$InsP_5$ could be a useful practical tool.

Conclusion

Ins(1,3,4,5,6)P_5 and its C-2 epimer *scyllo*-$InsP_5$ were synthesised from the same *myo*-inositol-based precursor and their conformational and protonation behaviours were compared by using potentiometric and NMR titrations. The results show that, over the physiological pH range, the acid–base properties and inositol-ring conformation of Ins(1,3,4,5,6)P_5 and *scyllo*-$InsP_5$ are similar, and that at pH 7.5, the same triprotonated and tetraprotonated species of each compound predominate with only small differences in their populations. These results suggest that *scyllo*-$InsP_5$ can be a useful tool for biological studies of Ins(1,3,4,5,6)P_5, because under experimental conditions where delocalised electrostatic interactions result in nonspecific effects, the two pentakisphosphates should behave in a similar way. In contrast, when Ins (1,3,4,5,6)P_5 and *scyllo*-$InsP_5$ are demonstrated to have different biological effects, then stereospecific binding sites that require the characteristic axial 2-OH group of Ins(1,3,4,5,6) P_5 are likely to be involved. This concept is illustrated by our demonstration that *scyllo*-$InsP_5$, unlike Ins(1,3,4,5,6)P_5, is neither dephosphorylated by PTEN nor phosphorylated by several Ins(1,3,4,5,6)P_5 2-kinases; this points to the importance of the axial 2-OH group in substrate recognition by these enzymes. In contrast, MINPP was able to dephophosphorylate both pentakisphosphates; this shows that, in this case, substrate recognition does not require the axial 2-OH group of Ins(1,3,4,5,6)P_5.

Experimental Section

Synthesis

General synthetic methods were carried out as previously reported.[21]

2,4-Di-O-(*p*-methoxybenzyl)-1,3,5-*O*-methylidyne-*scyllo*-inositol (5)

Sodium borohydride (430 mg, 11.6 mmol) was added in portions to a stirred solution of ketone **4**[21] (1.98 g, 4.63 mmol) in a mixture of THF (20 mL) and methanol (80 mL) at room temperature. After 30 min, TLC (ethyl acetate/hexane, 1:1) showed complete conversion of **4** (streak on TLC plate) into a single product (R_f 0.44). Water (100 mL) was added and the product was extracted with dichloromethane (3 0 100 mL). The combined organic extracts were washed with brine, dried ($MgSO_4$) and concentrated to give a white solid, which was recrystallised from ethyl acetate/hexane, to give alcohol **5** (1.77 g, 4.12 mmol, 89%); m.p. 125–126 °C (from ethyl acetate/hexane). ^{1}H NMR (270 MHz, $CDCl_3$): δ = 3.79 (s, 6H; 2 OCH_3), 4.10 (d, D_2O exch., ^3J**(H,H)** = 12.45 Hz, 1 H; OH), 4.34–4.42 (m, 3 H; H-6; 2 inositol H), 4.43–4.48 (m, 2 H; 2 inositol H), 4.56 (s, 4 H; OCH_2Ar), 4.56 (m, buried, 1 H; H-3), 5.49 (s, 1 H; O_3CH), 6.77–6.84 (m, 4 H; C_6H_4OMe), 7.08–7.16 (m, 4H; C_6H_4OMe); elemental analysis calcd (%) for $C_{23}H_{26}O_8$ (430.45): C 64.18, H 6.09; found: C 63.9, H 6.08.

6-*O*-Benzyl-2,4-di-O-(*p*-methoxybenzyl)-1,3,5-*O*-methylidyne-*scyllo*-inositol (6)

Sodium hydride (400 mg of a 60% suspension in oil, 10 mmol) was added to a solution of alcohol **5** (2.15 g, 5.00 mmol) in dry DMF at room temperature. After 30 min, the suspension was cooled to 0 °C and benzyl bromide (0.7 mL, 6 mmol) was added dropwise over 5 min. The mixture was allowed to reach room temperature and stirred overnight. Excess NaH was destroyed by careful addition of water and the solvents were removed by evaporation under reduced pressure. The residue was partitioned between dichloromethane and water (100 mL of each), the organic layer was separated, dried ($MgSO_4$) and concentrated to give an oily residue. Purification by flash chromatography (ethyl acetate/hexane, 1:4 then 1:3) gave **6** (2.31 g, 4.44 mmol, 89%) as a white solid; m.p. 106–107 °C (from ethyl acetate/hexane). ^{1}H NMR (400 MHz, $CDCl_3$): δ = 3.76 (s, 6 H; 2 OCH_3), 4.27–4.32 (m, 3 H; 3 inositol H), 4.47–4.52 (m, 3 H; 3 inositol H), 4.53 (s, 4 H; OCH_2Ar), 4.59 (s, 2H; OCH_2Ph), 5.49 (s, 1 H; O_3CH), 6.66–6.69 (m, 4 H; C_6H_4OMe), 7.10–7.13 (m, 4 H; C_6H_4OMe), 7.15–7.24 (m, 5H; Ph); elemental analysis calcd (%) for $C_{30}H_{32}O_8$ (520.57): C 69.22, H 6.20; found: C 69.5, H 6.23.

1-*O*-Benzyl-*scyllo*-inositol (7)

A suspension of **6** (1.56 g, 3.00 mmol) in ethanol (30 mL) and HCl (1.0 M, 15 mL) was heated at reflux for 4 h. When the clear solution was allowed to cool to room temperature, crystals of pentaol **7** appeared. The crystals were removed by filtration, washed well with ethanol and dried in vacuo at 60°C to give pure **7** (667 mg, 2.47 mmol, 82%). The crystals sublimed above 220 °C to give new crystals on the cover slip, m.p. 270–272°C. ^{1}H NMR (270 MHz, [D_6] DMSO): δ = 2.92–3.08 (m, 4H; 4 inositol H), 3.16 (ddd, ^3J**(H,H)** = 8.4, 8.2, 4.5 Hz, 2H; 2 inositol H), 4.73 (d, ^3J**(H,H)** = 3.2 Hz, 1H; OH-4), 4.77 (s, 2H; OCH_2Ph), 4.78 (d, ^3J**(H,H)** = 4.2 Hz, 2H; 2 OH), 4.84 (d, ^3J**(H,H)** = 4.7 Hz, 2 H; 2OH), 7.20–7.34 (m, 3H, Ph), 7.38–7.45 (m, 2 H, Ph); elemental analysis calcd (%) for $C_{13}H_{18}O_6$ (270.3): C 57.77, H 6.71; found: C 57.8, H 6.70.

1-*O*-Benzyl-*scyllo*-inositol 2,3,4,5,6-pentakis(dibenzylphosphate) (8)

A solution of 1*H*-tetrazole (10 mL of a 0.45M solution in acetonitrile, 4.5 mmol) was added to finely powdered pentaol **7** (135 mg, 0.500 mmol) under N_2, followed by bis(benzyloxy) diisopropylaminophosphine (1.3 mL, 3.75 mmol). The mixture was stirred at room temperature for 1.5 h and the solvents were then removed by evaporation under reduced pressure. The residue was taken up in dichloromethane (10 mL) and cooled to −78°C before addition of 3-chloroperoxybenzoic acid (60 %, 1.4 g, 5.0 mmol). The mixture was allowed to warm to room temperature, then diluted with dichloromethane (50 mL), washed with aqueous Na_2SO_3 (10 %) and dried over $MgSO_4$. Evaporation, followed by flash chromatography on silica (ethyl acetate/hexane (1:2) then ethyl acetate) gave **8** as an oil (543 mg, 0.346 mmole, 69%). ^{1}H NMR (270 MHz, $CDCl_3$): δ = 4.16 (t, ^3J**(H,H)** = 4.7 Hz, 1 H; H-1), 4.61 (s, 2H; OCH_2Ph), 4.84–5.16 (m, 25H; H-2, H-3, H-4, H-5, H-6, 10OCH_2Ph), 7.12–7.32 (m, 55H; 11Ph); ^{31}P NMR (100 MHz, $CDCl_3$, ^{1}H-decoupled): δ = −1.34 (2 P), −1.31 (2 P), −1.20 (1 P). High resolution MS-FAB (positive ion): calcd $C_{83}H_{84}O_{21}P_5^+$: 1571.4193; found: 1571.4172.

scyllo-Inositol 1,2,3,4,5-pentakisphosphate (2) [15]

Palladium on activated charcoal (Aldrich; 10%, 50% water, 1.0 g) was added to a solution of **8** (500 mg, 0.318 mmol) in methanol (60 mL) and deionised water (10 mL). The mixture was shaken in a Parr hydrogenator under an atmosphere of hydrogen (3.5 bar) for 24 h. The catalyst was removed by filtration through a PTFE syringe filter and the solution was neutralised by the addition of triethylammonium bicarbonate (TEAB) buffer (1 M, 2 mL). The solvents were removed by evaporation under reduced pressure. The residue was purified by ion-exchange chromatography on Q-Sepharose fast-flow resin and eluted with a gradient of TEAB buffer (0 to 1.5 M over 950 mL, collecting 10 mL fractions). Fractions were tested for phosphate by using

a modification of the Briggs phosphate assay.[31] The target compound (**2**) eluted at a concentration of 80% buffer. Fractions containing **2** were combined and concentrated by evaporation under reduced pressure. Methanol was repeatedly added and evaporated to decompose excess TEAB until a clear colourless glass remained. Lyophilisation of this residue from deionised water gave the pure triethylammonium salt of **2** as a colourless glassy solid (0.233 mmol as determined by total phosphate assay, 73%). ^{1}H NMR (270 MHz, CD_3OD): δ = 3.56 (t, ^3J**(H,H)** = 9.2 Hz, 1 H; H-6), (ddd, ^3J**(H,H)** = 9.4, 9.2 Hz, ^3J**(H,P)** = 9.1 Hz, 2H; 2 inositol H); 4.18–4.30 (m, 3H; 3 inositol H); ^{31}P NMR (109 MHz, CD_3OD, ^{1}H-decoupled): δ = 1.44 (2 P), 1.67 (2 P), 1.96 (1P); high-resolution mass MS-FAB (negative ion) calcd for $C_6H_{16}O_{21}P_5^-$: 578.8872; found: 578.8871.

2-*O*-Benzyl-4,6-di-O-(*p*-methoxybenzyl)-1,3,5-*O*-methylidyne-*myo*-inositol (9)

Benzylation of alcohol **3**[21] (as described for **5**) and purification by flash chromatography (ethyl acetate/hexane, 1:3) gave **9** as an oil, which slowly crystallised; m.p. 57–59 °C (from ether). ^{1}H NMR (270 MHz, $CDCl_3$): δ = 3.80 (s, 6 H; $2OCH_3$), 3.98–4.02 (m, 1 H; H-2), 4.23–4.27 (m, 2H; H-1/3), 4.29 (dd, ^3J**(H,H)** = 3.9, 3.5 Hz, 2 H; H-4/6), 4.37 (m, buried, 1 H; H-5), 4.39, 4.52 (AB system, ^2J**(H,H)** = 11.1 Hz, 4 H; OCH_2Ar), 4.63 (s, 2H; OCH_2Ph), 5.52 (d, ^5J-**(H,H)** = 1.3 Hz, 1 H; O_3CH), 6.78–6.84 (m, 4 H; C_6H_4OMe), 7.08–7.15 (m, 4H; C_6H_4OMe), 7.27–7.40 (m, 5H; Ph); elemental analysis: calcd for $C_{30}H_{32}O_8$ (520.57): C 69.22, H 6.20; found: C 69.3, H 6.22.

2-*O*-Benzyl-*myo*-inositol (10)

A suspension of **9** (1.56 g, 3.00 mmol) in ethanol (30 mL) and HCl (1.0 M, 15 mL) was heated at reflux for 4 h and then allowed to cool. Crystals of pentaol were isolated in the same way as for **7**, to give **10** (547 mg, 2.07 mmol, 67%); the crystals sublimed above 200°C to give new crystals on the cover slip, m.p. 248–251 °C; ref. [23a]: m.p. 248–250°C (dec); ref. [32]: m.p. 250–251 °C. ^{1}H NMR (270 MHz, [D_6]DMSO): δ = 2.93 (td, ^3J**(H,H)** = 8.9, 4.5 Hz, 1H; H-5), 3.26 (ddd, ^3J**(H,H)** = 9.6, 4.5, 2.5 Hz, 2 H; H-1/3), 3.39 (ddd, ^3J**(H,H)** = 9.4, 9.1, 4.5 Hz, 2 H; H-4/6), 3.71 (t, ^3J**(H,H)** = 2.5 Hz, 1 H; H-2), 4.64–4.67 (m, 5 H; 5OH), 4.76 (s, 2 H; OCH_2Ph), 7.21–7.34 (m, 3H; Ph), 7.37–7.43 (m, 2H; Ph); elemental analysis calcd (%) for $C_{13}H_{18}O_6$ (270.3): C 57.77, H 6.71; found: C 57.5, H 6.65.

2-*O*-Benzyl-*myo*-inositol 1,3,4,5,6-pentakis(dibenzylphosphate) (11):[23a]

Phosphitylation of **10** (203 mg, 0.75 mmol) followed by oxidation and purification (as described in the synthesis of **8**) gave **11** as a colourless oil (932 mg, 0.593 mmol, 79%). ^{1}H NMR (400 MHz, $CDCl_3$): δ = 4.27 (ddd, ^3J**(H,H)** = 9.8, 2.3 Hz, ^3J**(H,P)** = 9.8 Hz, 1 H; H-1/3), 4.38 (dt, ^3J**(H,P)** = 9.8 Hz, ^3J**(H,H)** = 9.4 Hz, 1 H; H-5), 4.73 (t, ^3J-**(H,H)** = 2.3 Hz, 1H; H-2), 4.75 (s, 2 H; OCH_2Ph), 4.87–5.07 (m, 22H; $10POCH_2Ph$, H-4/6), 7.12–7.26 (m, 55 H; 11 Ph); ^{31}P NMR (162 MHz, $CDCl_3$, ^{1}H-decoupled) δ = −0.87 (2 P), −0.18 (2 P), 0.15 (1P); elemental analysis calcd (%) for $C_{83}H_{83}O_{21}P_5$ (1571.4): C 63.44, H 5.32; found: C 63.5, H 5.31.

myo-Inositol 1,3,4,5,6-pentakisphosphate (1):[23]

Hydrogenolytic deprotection of **11** (540 mg, 0.344 mmol) and purification (as described for **2**) gave the pure triethylammonium salt of **1** as a colourless glassy solid (0.220 mmol as determined by total phosphate assay, 64 %). ^{1}H NMR (400 MHz, CD_3OD) δ = 4.13 (ddd, ^3J**(H,H)** = 9.7, 2.3 Hz, ^3J**(H,P)** = 9.8 Hz, 2 H; H-1/3), 4.18 (dt, ^3J**(H,P)** = 9.8 Hz, ^3J-**(H,H)** = 9.4 Hz, 1 H; H-5), 4.29 (t, ^3J**(H,H)** = 2.3 Hz, 2H; H-2), 4.62 (ddd, ^3J**(H,P)** = 9.7 Hz, ^3J**(H,H)** = 9.7, 9.4 Hz, 2 H; H-4/6); ^{31}P NMR (162 MHz, CD_3OD, ^{1}H-decoupled): δ = 1.18 (2 P), 2.00 (2 P), 2.25 (1 P).

Potentiometric studies and NMR determinations

Potentiometric and NMR experiments were performed in two steps, in which the same initial solution of the studied compounds (about 2 mM) was successively subjected to potentiometric and ^{31}P or ^{1}H NMR titrations. The processing of the pH measurements allowed the total concentration of the ligand and the acid as well as the macroscopic protonation constants (by using HYPERQUAD) to be determined. The NMR titrations were performed on 0.50 mL of solution in D_2O on a Bruker DPX-300 Fourier transform spectrometer. One-dimensional ^{31}P NMR spectra were recorded at 121.50 MHz and ^{31}P chemical-shifts values were referenced to an external 85 % H_3PO_4 signal at 0.00 ppm with downfield shifts represented by positive values. Spectra were acquired over a spectral width of 10 ppm by using a 0.1 s relaxation delay and a $\pi/2$ pulse. Typically 1 K data points were sampled with a corresponding 0.4 s acquisition time. The spectra had a digital resolution of 1.19 Hz per point. ^{1}H NMR spectra were acquired with water presaturation over a spectral width of 6 ppm by using a 3 s relaxation delay and a $\pi/2$ pulse. 4 K data points were sampled with a corresponding 1.14 s acquisition time. The spectra had a digital resolution of 0.44 Hz per point. Data were zero filled and a 1 Hz exponential line broadening function was applied prior to Fourier transformation. The temperature in both cases was controlled at 37 ± 0.5 °C. The proton and phosphorus resonances of Ins(1,3,4,5,6)P_5 and *scyllo*-InsP_5 were assigned by performing proton–proton and phosphorus–proton 2D correlation experiments with at least two suitable pH values, this allowed the titration curves to be unambiguously characterized. Cluster and chemical-shift parameters, which were used to calculate the conditional probabilities (Figure 4), were obtained by a nonlinear least-squares fitting procedure to the chemical-shift data. More details of the fitting procedure are provided elsewhere.[25, 33,34]

Cloning of human Ins(1,3,4,5,6)P_5 2-kinase

The gene encoding human Ins(1,3,4,5,6)P_5 2-kinase was amplified by PCR by using a TrueClone human full-length cDNA clone (OriGene) as template. The upstream primer was 5′-GGGGACAAGTAGTTTGTACAAAAAAGCAGGCACCATGGAAGAGGGGAAGATGGACG-3′, and the downstream primer was 5′-GGGGACCACTTTGTACAAGAAAGCTGGTTAGACCTTGTGGAGAACTAATG-3′. The PCR product was cloned into pDONR vector (Invitrogen) which was subsequently used to construct pDEST605-hIP2kinase by using the manufacturer's instructions.

Purification of human Ins(1,3,4,5,6)P_5 2-kinase from Sf9 cells

The pDEST605-hIP2kinase vector containing the full length human Ins(1,3,4,5,6)P_5 2-kinase was used to generate bacmid insect viral DNA (Invitrogen). The His-tagged fusion protein was expressed in Sf9 cells by using the baculovirus expression system (Invitrogen). Cells were infected for 3 days and then lysed in lysis buffer (Promega). The lysate was allowed to bind to Ni Sepharose high performance beads (Amersham Biosciences), washed with HEPES pH 7.3 buffer and eluted with imidazole (200 mM) gradient buffer. The peak elute was run on an SDS-PAGE gel and stained with Simply Blue stain (Invitrogen) and a single protein band of ~60000 kDa was identified.

Expression and purification of recombinant *Arabidopsis* Ins(1,3,4,5,6)P_5 2-kinase

The 2-kinase plasmid (kindly provided by Drs. John York and Stevenson-Paulik, Duke University, NC, USA) was transformed into DH5 *E. coli* competent cells. DH5 *E. coli* cells (1 L) were grown overnight at 28°C to an absorbance of ~0.6 at 595 nm. Gene expression was induced by addition of IPTG (1.0 mM). The cells were continuously cultured for 4 h, harvested and frozen at −80 °C. Frozen cells were thawed at 4 °C and added to lysis buffer (PBS pH 7.4, NP40 0.05 %, PMSF 1 mM). The lysate was cleaned by centrifugation at 15000*g* for 15 min at

4°C and the supernatant was incubated with glutathione–Sepharose resin (1 mL, 50%) for 15 min at room temperature. The Sepharose was washed three times with PBS buffer and the GST fusion protein was eluted with reduced glutathione (1 mL, 10 mM) three times. Each eluate was kept at −80°C in aliquots.

Enzyme-assay conditions

Ins(1,3,4,5,6)P_5 2-kinase assays were performed by a slight modification of the procedure described in ref. [35]. Either Ins(1,3,4,5,6)P_5 or *scyllo*-InsP_5 (50 μM) was incubated with purified recombinant 2-kinase (1.0 μg) from either *Arabidopsis*, *H. sapiens* or *S. cerevisiae* in buffer (10 μL) containing HEPES (20 mM, pH 7.3), KCl (100 mM), $MgSO_4$ (15 mM) and γ-^{32}P-ATP (0.5 μL, 300 000 cpm) for 5 h at 37°C. Assays were quenched, neutralized and analyzed on a 12.50 4.6 mm Partisphere SAX HPLC column eluted with an ammonium phosphate gradient as previously described.[36] The radioactivity was assessed “online” by using a Flo-1 counter (Packard Instruments) with a 1:3 mixture of HPLC eluate/scintillation fluid (MonoFlo4, National Diagnostics). Data were acquired by using Flo-1 for Windows (v3.61) and then exported as an ASCII file into SigmaPlot (v8.0).

Recombinant human PTEN and MINPP were obtained as previously described (see refs. [9] and [37], respectively). These enzymes were incubated in buffer (100 μL) containing Tris–HCl (50 mM, pH 7.2). Enzyme activity was determined against Ins(1,3,4,5,6)P_5 (25 μM) at 37°C by using a phosphate-release assay.[38]

Molecular docking of Ins(1,3,4,5,6)P_5 into the active site of PTEN

Molecular-docking experiments were carried out according to general methods previously described.[39] By using the SYBYL 7.0 program (Tripos Associates) Ins(1,3,4,5,6)P_5 was extracted from the crystal structure of the PH domain of GRP1 (PDB ID: 1FHW; ligand identifier I5P1001). The crystal structure of PTEN was obtained from the Brookhaven Protein Data Bank (PDB ID: 1D5R). The GOLD docking program (v2.2)[40] was used to dock the flexible model of Ins(1,3,4,5,6)P_5 into the PTEN active site, which was defined as a 10 & sphere around the Sγ atom of Cys124. The ligand was docked to the enzyme a total of 40 times and the docking modes that achieved the highest fitness score were retained and compared. The predicted position of Ins(1,3,4,5,6)P_5 in the PTEN binding site (Figure 5) resembles earlier predictions[9] made by superimposing the 3- and 4-phosphate groups of a rigid model of Ins (1,3,4,5,6)P_5 on the bound L-(+)-tartrate molecule of the X-ray structure; although, in the GOLD-docked model some interactions of phosphate groups with conserved active-site residues, predicted by mutagenesis studies,[29] are better reproduced. The scissile 3-phosphate group of Ins(1,3,4,5,6)P_5 is well positioned for nucleophilic attack by Cys124 (not shown) and for stabilising interactions with the electrostatic dipole of a nearby α-helix. Figure 5 was produced by using PyMOL (http://www.pymol.org)

Acknowledgements

We thank the Wellcome Trust for Programme Grant support (060554 to B.V.L.P.). Recombinant Ins(1,3,4,5,6)P_5 2-kinase from *S. cerevisiae* was kindly provided by Dr. John York and Dr. Andrew Seeds. We also thank the Commissariat 3 l’Energie Atomique (CEA) and the Conseil Régional d’Alsace for a Ph.D fellowship (P.K.).

References

1. S. B. Shears in The Handbook of Cell Signalling, Vol. 2 (Eds.: R. Bradshaw, E. Dennis), Academic Press, San Diego, 2003, pp. 233–236.
2. Orchiston EA, Bennett D, Leslie NR, Clarke RG, Winward L, Downes CP, Safrany ST. J Biol Chem 2004;279:1116–1122. [PubMed: 14561749]
3. Piccolo E, Vignati S, Maffucci T, Innominato PF, Riley AM, Potter BVL, Pandolfi PP, Broggini M, Iacobelli S, Innocenti P, Falasca M. Oncogene 2004;23:1754–1765. [PubMed: 14755253]

4. Campbell S, Fisher RJ, Towler EM, Fox S, Issaq HJ, Wolfe T, Phillips LR, Rein A. Proc Natl Acad Sci USA 2001;98:10 875–10 879.
5. Steger DJ, Haswell ES, Miller AL, Wente SR, O'Shea EK. Science 2003;299:114–116. [PubMed: 12434012]
6. Quignard JF, Rakotoarisoa L, Mironneau J, Mironneau C. J Physiol 2003;549:729–737. [PubMed: 12717004]
7. Maffucci T, Piccolo E, Cumashi A, Iezzi M, Riley AM, Saiardi A, Godage HY, Rossi C, Broggini M, Iacobelli S, Potter BVL, Innocenti P, Falasca M. Cancer Res 2005;65:8339–8349. [PubMed: 16166311]
8. Komander D, Fairservice A, Deak M, Kular GS, Prescott AR, Downes CP, Safrany ST, Alessi DR, van Aalten DMF. EMBO J 2004;23:3918–3928. [PubMed: 15457207]
9. Caffrey JJ, Darden T, Wenk MR, Shears SB. FEBS Lett 2001;499:6–10. [PubMed: 11418101]
10. Irvine RF, Schell MJ. Nat Rev Mol Cell Biol 2001;2:327–338. [PubMed: 11331907]
11. Ho MWY, Shears SB. Curr Top Membr 2002;53:345–363.
12. Lemmon MA, Ferguson KM, Abrams CS. FEBS Lett 2002;513:71–76. [PubMed: 11911883]
13. Shears SB. Cell Signal 2001;13:151–158. [PubMed: 11282453]
14. Lemtiri-Chlieh F, MacRobbie EAC, Brearley CA. Proc Natl Acad Sci USA 2000;97:8687–8692. [PubMed: 10890897]
15. Chung SK, Kwon YU, Chang YT, Sohn KH, Shin JH, Park KH, Hong BJ, Chung IH. Bioorg Med Chem 1999;7:2577–2589. [PubMed: 10632068]
16. Horne G, Maechling C, Fleig A, Hirata M, Penner R, Spiess B, Potter BVL. Biochem Biophys Res Commun 2004;320:1262–1270. [PubMed: 15249226]
17. Verbsky JW, Wilson MP, Kisseleva MV, Majerus PW, Wente SR. J Biol Chem 2002;277:31 857–31 862.
18. Stevenson-Paulik J, Bastidas RJ, Chiou ST, Frye RA, York JD. Proc Natl Acad Sci USA 2005;102:12 612–12 617.
19. Shears SB. Biochem J 2004;377:265–280. [PubMed: 14567754]
20. Turner BL, Paphazy MJ, Haygarth PM, McKelvie ID. Philos Trans R Soc London Ser B 2002;357:449–469. [PubMed: 12028785]
21. Riley AM, Guedat P, Schlewer G, Spiess B, Potter BVL. J Org Chem 1998;63:295–305.
22. Lee HW, Kishi Y. J Org Chem 1985;50:4402–4404.
23. Lu PJ, Gou DM, Shieh WR, Chen CS. Biochemistry 1994;33:11586–11 597. [PubMed: 7918372]a) Ozaki S, Koga Y, Ling L, Watanabe Y, Kimura Y, Hirata M. Bull Chem Soc Jpn 1994;67:1058–1063.b)Chung SK, Chang YT. Bioorg Med Chem Lett 1996;6:2039–2042.c)Rudolf MT, Kaiser T, Guse AH, Mayr GW, Schultz C. Liebigs Ann/Recl 1997:1861–1869.d)Podeschwa MAL, Plettenburg O, Altenbach HJ. Eur J Org Chem 2005:3101–3115.e)
24. Barrientos LG, Murthy PPN. Carbohydr Res 1996;296:39–54. [PubMed: 9008842]
25. Borkovec M, Koper GJM. Anal Chem 2000;72:3272–3279.
26. Nogimori K, Hughes PJ, Glennon MC, Hodgson ME, Putney JW, Shears SB. J Biol Chem 1991;266:16 499–16 506.
27. Ballereau S, Guédat P, Poirier SN, Guillemette G, Spiess B, Schlewer G. J Med Chem 1999;42:4824–4835. [PubMed: 10579845]
28. Felemez M, Bernard P, Schlewer G, Spiess B. J Am Chem Soc 2000;122:3156–3165.
29. Lee JO, Yang HJ, Georgescu MM, Di Cristofano A, Maehama T, Shi YG, Dixon JE, Pandolfi P, Pavletich NP. Cell 1999;99:323–334. [PubMed: 10555148]
30. Jackson MD, Denu JM. Chem Rev 2001;101:2313–2340. [PubMed: 11749375]Reviewed in; a)Bialy L, Waldmann H. Angew Chem 2005;117:3880–3906.b)Angew. Chem. Int. Ed. 2005, 44, 3814–3839;Dewang PM, Hsu NM, Peng SZ, Li WR. Curr Med Chem 2005;12:1–22. [PubMed: 15638728] c)
31. Lampe D, Liu CS, Potter BVL. J Med Chem 1994;37:907–912. [PubMed: 8151617]
32. Sureshan KM, Shashidhar MS, Praveen T, Gonnade RG, Bhadbhade MM. Carbohydr Res 2002;337:2399–2410. [PubMed: 12493224]

33. Borkovec M, Spiess B. Phys Chem Chem Phys 2004;6:1144–1151.
34. Kuad P, Borkovec M, Murr MDE, Le Gall T, Mioskowski C, Spiess B. J Am Chem Soc 2005;127:1323–1333. [PubMed: 15669874]
35. Stevenson-Paulik J, Odom AR, York JD. J Biol Chem 2002;277:42 711–42 718.
36. Saiardi A, Caffrey JJ, Snyder SH, Shears SB. J Biol Chem 2000;275:24 686–24 692.
37. Deleu S, Choi K, Pesesse X, Cho J, Sulis ML, Parsons R, Shears SB. Cell Signal 2006;18:488–498. [PubMed: 15979280]
38. Ullah AHJ, Sethumadhavan K, Mullaney EJ, Ziegelhoffer T, Austin-Phillips S. Biochem Biophys Res Commun 1999;264:201–206. [PubMed: 10527865]
39. Rosenberg HJ, Riley AM, Laude AJ, Taylor CW, Potter BVL. J Med Chem 2003;46:4860–4871. [PubMed: 14584937]
40. Jones G, Willett P, Glen RC, Leach AR, Taylor R. J Mol Biol 1997;267:727–748. [PubMed: 9126849]

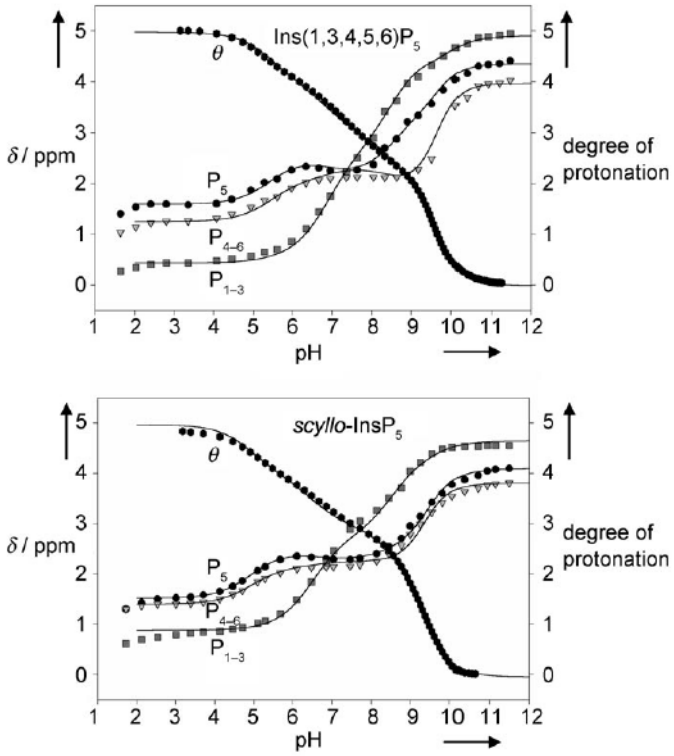

Figure 1.

^{31}P NMR titrations curves [δ = f(pH)] for Ins(1,3,4,5,6)P_5 and *scyllo*-InsP_5 along with the potentiometric site-specific degree of protonation [θ = f(pH)] determined in 0.2 M KCl at 37 °C (D_2O). Least-squares fits are shown as solid lines; see text for details.

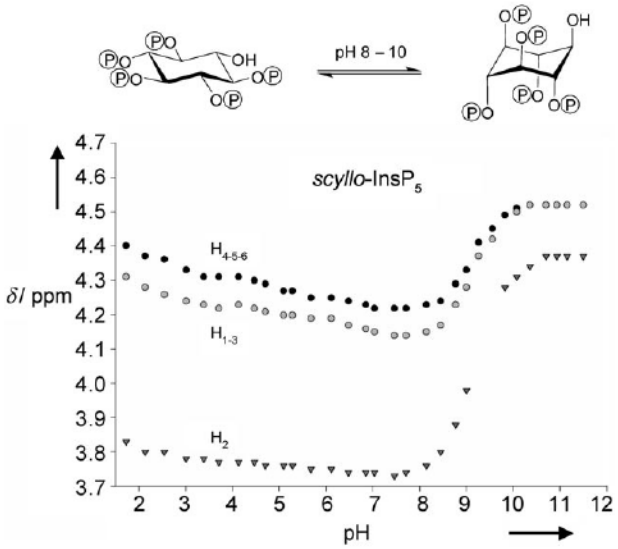

Figure 2.

^{1}H NMR titrations curves for *scyllo*-InsP_5 (0.2 M KCl at 37 °C in D_2O) show that pH-dependent inositol ring flipping occurs over the pH range 8–10.

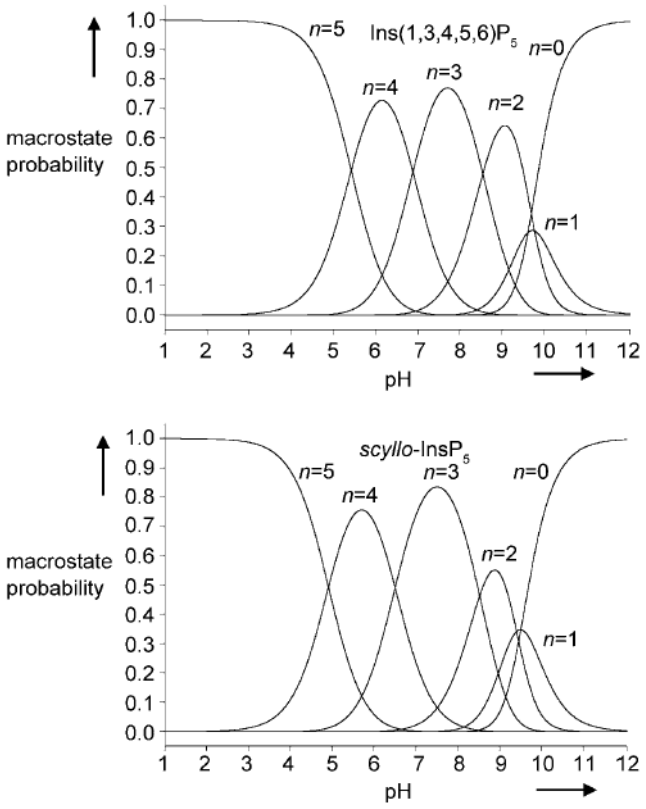

Figure 3.

Macrostate probabilities for Ins(1,3,4,5,6)P_5 and *scyllo*-InsP_5 (0.2 M KCl at 37 °C in D_2O) calculated from the potentiometric titration curves in Figure 1.

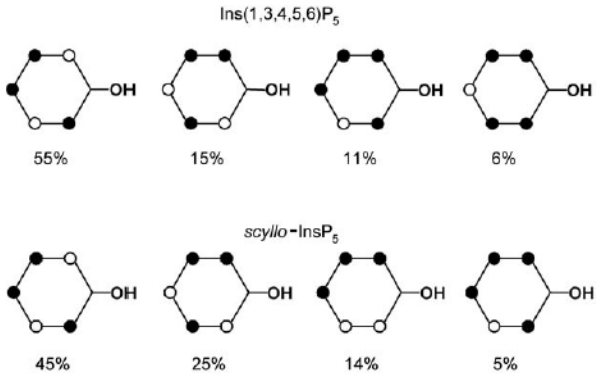

Figure 4.
Conditional probabilities (%) for Ins(1,3,4,5,6)P_5 and *scyllo*-InsP_5 at pH 7.5; • : protonated sites.

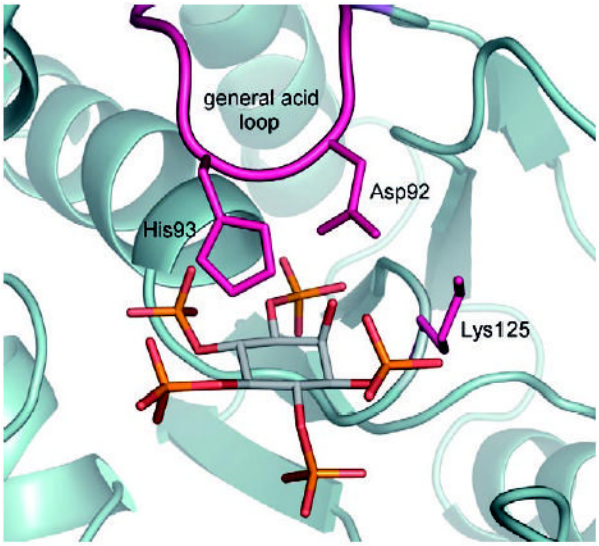

Figure 5.

Model of Ins(1,3,4,5,6)P_5 docked into the catalytic site of PTEN (PDB ID: 1D5R). The axial 2-OH group of Ins(1,3,4,5,6)P_5 is predicted to be close to Asp92 of the general acid loop, which is thought to be involved in the mechanism of catalysis.[9,29] The 2-OH group might also influence the conformation of the 1-phosphate group, which is predicted to have stabilising interactions with Lys125. For details, see Experimental Section and Discussion. For clarity, hydrogen atoms are not shown.

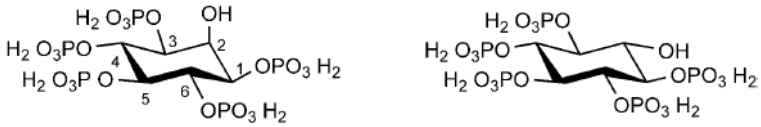

Ins(1,3,**4**,5,6)P_5 (**1**) *scyllo*-InsP_5 (**2**)

Scheme 1.

Structures of *myo*-inositol 1,3,4,5,6-pentakisphosphate (Ins(1,3,4,5,6)P_5, **1**) and s*cyllo*-inositol pentakisphosphate (*scyllo*-InsP_5, **2**).

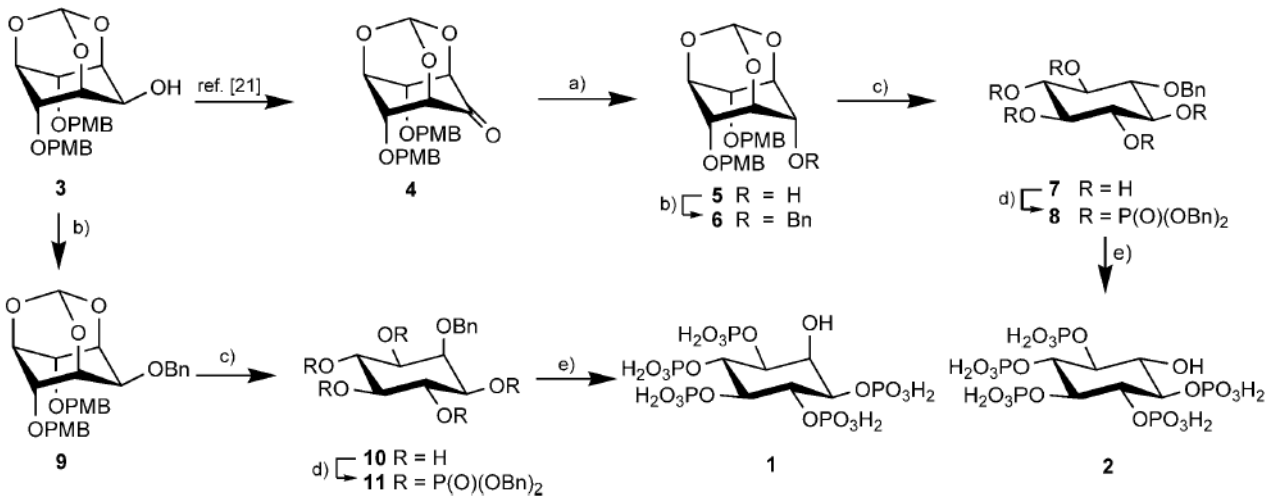

Scheme 2.

Synthesis of Ins(1,3,4,5,6)P_5 (**1**) and s*cyllo*-InsP_5 (**2**). Reagents and conditions: a) $NaBH_4$, THF, MeOH; b) BnBr, NaH, DMF; c) 1.0 M HCl/EtOH (1:2), reflux; d) i. $(BnO)_2PNPr^i_2$, 1*H*-tetrazole, CH_3CN; ii. *m*CPBA, CH_2Cl_2, −78°C to room temperature; e) Pd-C, MeOH, H_2O, H_2, 3.5 bar; Bn = benzyl, PMB = 4-methoxybenzyl.